Counterion and Coion Distribution Functions in the Counterion Condensation Theory of Polyelectrolytes

Jolly Ray and Gerald S. Manning*

Department of Chemistry, Rutgers University, 610 Taylor Road, Piscataway, New Jersey 08854-8087

Received February 17, 1999; Revised Manuscript Received May 3, 1999

ABSTRACT: We develop formulas for the counterion−polyion and coion−polyion potentials of mean force in the context of counterion condensation theory. For separation distances on the scale of a Debye screening length, both potentials conform to Debye−Hückel screening behavior. Close to the polyion, in the region defining the layer of condensed counterions, the counterion potential is attractive and unscreened. A coion in this region acts like a charged group on the polyion; its potential is repulsive, and it augments the ability of the polymer to condense counterions. There is an interfacial region between condensed layer and diffuse cloud from which counterions are expelled back into the cloud but which accumulates coions. The associated radial distribution functions exhibit two peaks for the counterion and a single peak for the coion.

1. Introduction

The counterion condensation theory of polyelectrolyte behavior rests on a model that allows the possibility of renormalization of the polyion charge to a value lower than the actual structural charge carried by the chain.[1−3] If the structural charge per unit chain length (contour length charge density) exceeds a certain threshold value that is independent of both the actual structural charge carried by the chain and the ionic strength of the solution, free energy optimization then determines a renormalized charge density equal to the threshold value. The physical mechanism of charge renormalization operates through the condensation of counterions on the chain until the net chain charge, including the charge of the condensed counterions, equals the renormalized charge. The renormalized charge is not zero, so some counterions remain uncondensed, and they are modeled as residing in a diffuse Debye−Hückel cloud surrounding the renormalized polyion.

The condensed counterions are not part of the covalent structure of the polyion chain. Nevertheless, they must be intimately involved with the chain structure, since they are as effective in determining the net charge on the polyion as the covalently attached ionized groups themselves. Recent neutron scattering data support this argument,[4] as do numerous other measurements and some simulations indicating sharp transitions at the threshold charge density.[1] The graphics accompanying a report of all-atom modeling of DNA with its counterions include the striking image of a double-helical array of mobile but condensed Na^+ ions visually distinct from a diffuse featureless distribution of uncondensed counterions.[5]

If the condensed counterions are actually part of a complex consisting of the polymer chain and closely held counterions and solvent molecules, an accurate and detailed determination of their distribution by analytical theory will be no easy task. Nevertheless, to the extent that a theory can help provide interpretive insight into the meaning of experimental and simulated data, it is worth the effort, even if modeling idealizations are necessary for the sake of tractability. In this paper, we find simplified formulas that have in fact helped us to understand why counterions are able to divide into two spatially distinct populations in the presence of a polymer of sufficiently high charge density.

2. Theory

2.1. Asymptotic Space. We consider a counterion or coion located at distance r from a polyion, modeled as a line of discrete charged sites. Each point in the space surrounding the polyion corresponds to some value of r, and we divide r-space into three regions: near, intermediate, and far.[6,7] The regions are defined asymptotically with respect to the limit $\kappa \to 0$, or $\kappa^{-1} \to \infty$, where κ is the Debye−Hückel screening parameter and κ^{-1} is the Debye length. The far region consists of points r that are $O(\kappa^{-1})$, values of r in the near region are $O(1)$, and intermediate values of r are $O(\kappa^{-x})$, where x is a fraction between 0 and 1.

A value of r in the far region recedes asymptotically to infinity in such a way that the product κr remains constant when $\kappa \to 0$. Choosing a continuum of values for the constant allows one to fill a volume region of asymptotically far space. A value of r in the near region is itself equal to a constant, and again, the choice of a continuum of values for the constant fills near space. An intermediate value of r recedes to infinity but more slowly than κ^{-1}, in the sense that r/κ^{-1} is of order κ^{1-x} and therefore tends to zero.

Since κ^{1-x} does not have the units of length, we need an explicit formula for distance values r in the intermediate region. It is

$$r = r_0^{1-x}\kappa^{-x} \quad 0 < x < 1 \tag{1}$$

where r_0 is a constant distance, hence in the near region. Note that when x is close to zero, an intermediate r is close to r_0, hence close to the near region. Since κr_0 is small, r increases as x sweeps through the interval from 0 to 1 and approaches the far region distance κ^{-1} as x approaches unity. Thus, the intermediate range fills the space between near and far regions. Moreover, the outer boundary of the near region is at $r = r_0$, and the inner boundary of the far region is at $r = \kappa^{-1}$.

We have placed a cut-off $r = r_0$ on the outer extent of the near region, and to produce numerical plots of our potentials, we need a reasonable estimate of its value.

10.1021/ma9902091 CCC: $18.00
Published on Web 06/23/1999

Consider distances r satisfying the relation

$$r = -r_0 \ln \kappa r_0 \tag{2}$$

These values of r recede asymptotically to infinity; therefore, they are outside the constant distances of the near range. Nevertheless, since the logarithmic function increases more slowly than any power of its argument, they are asymptotically smaller than any distance in the intermediate range. The region therefore lies between the near and intermediate ranges. However, for a specified ionic strength corresponding to a finite Debye length κ^{-1}, we can bring the intermediate region right up to the near region by setting $x = 0$ in eq 1. The range described by eq 2 shrinks to the point $r = r_0$, separating near from intermediate distances, and we can get eq 2 to satisfy $r = r_0$ with the requirement,

$$r_0 = e^{-1}(1/\kappa) \tag{3}$$

Note that this estimate of r_0 is not an asymptotic formula (it would meaninglessly place r_0 in the far range if it were), since we have derived it for specified finite values of $1/\kappa$. Note as well that it provides the physically reasonable numerical requirement that the intermediate range be bounded by the values $r = 0.368(1/\kappa)$ and $r = 1/\kappa$. Given the usual qualitative meaning assigned to the factor e^{-1}, we can say that the outer boundary of the near region is where screening sets in. Ions located within this boundary are not screened from the polymer charge, and in this sense, their charge can be assigned to the net charge of a polymer−ion complex.

The behavior of the Bessel K-function of zeroth order as a function of its argument κr is central to our analysis. In the near and intermediate regions, $\kappa r = o(1)$, and we use the leading terms of an asymptotic expansion,

$$K_0(\kappa r) \approx -\ln\left(\frac{1}{2}\kappa r\right) - \gamma \tag{4}$$

where $\gamma = 0.5772...$ is the Euler constant. In contrast, κr in the far region is constant; so, there we will treat $K_0(\kappa r)$ as a constant.

2.2. Counterion−Polyion Potential. *2.2.1. Components of the Work.* We consider a counterion fixed at distance r from a polyion, modeled as a linear array of P renormalized point charges with spacing b. Each renormalized polymer charge equals $[1 - \theta(r)]q$, where q is the charge on an electron (proton) if the polymer is anionic (cationic). The quantity θ is a fraction between zero and unity expressing the renormalization of polymer charge. The extent of renormalization is to be determined by free energy minimization, and the value $\theta = 0$ is one of the possibilities. We also allow for the possibility that the extent of renormalization is influenced by the counterion at r, hence $\theta = \theta(r)$. The polymer and counterion at r are immersed in 1:1 electrolyte of bulk concentration c and screening parameter κ. In the following, it is understood that all work (free energy) terms are in units of k_BT, the product of Boltzmann constant and Kelvin temperature.

The work $w_p(r)$ required to assemble the polymer charges in the presence of the counterion at r, account taken only of the interactions among polymer charges, is obtained in our theory as the leading term in an electrolyte concentration expansion of the sum of screened Debye−Hückel (or Yukawa) potentials $\exp(-\kappa r_{ij})/r_{ij}$ over all pairs {ij} of renormalized charges in the linear array representing the polymer, $r_{ij} = nb$, where n is an integer. The result[2] is

$$w_p(r) = -[1 - \theta(r)]^2\, \xi P \ln(\kappa b) \tag{5}$$

where ξ is the dimensionless polymer charge density l/b, l is the Bjerrum length q^2/Dk_BT, and D is the dielectric constant of bulk solvent. The infinite series encountered in obtaining eq 5 is executed by standard mathematical software, or it can be done manually by integrating a geometric series.

The physical mechanism of renormalization is the condensation of counterions; thus, θ is the number of condensed counterions divided by P. The local energetics and structure of the condensed layer is characterized by an internal partition function Q that may be sensitive to the presence of the counterion at r: $Q = Q(r)$. The work required to transfer θP counterions from bulk solution to the condensed layer, exclusive of their interaction with the Debye−Hückel atmosphere (accounted for in eq 5), is given by the formula

$$w_{\text{transfer}}(r) = \theta(r)P \ln[10^3\theta(r)/cQ(r)] \tag{6}$$

which is simply the difference of two chemical potentials in standard logarithmic form.

Finally, there is the screened Debye−Hückel interaction between the counterion at r and a renormalized polymer charge, summed over all polymer charges, to give a contribution w_{cp} to the work. With the sum replaced by an integration, we have

$$w_{cp}(r) = -2Z\xi(1 - \theta)K_0(\kappa r) \tag{7}$$

where K_0 is the Bessel K-function of zeroth order and Z is the absolute value of the valence of the counterion (the bathing electrolyte is uni-univalent, but we take the fixed counterion as Z-valent with an eye to subsequent applications).

In the case of eq 5, the use of Debye−Hückel potentials is justified, because the important charge pairs occuring in the lattice sum are widely separated (by distances of order κ^{-1}), but our theory applies eq 7 at distances r close as well as far from the polyion. In this case, the application of eq 7 at close distances is justified by the results obtained from it. It gives rise to a spatially identifiable layer of condensed counterions, which in turn is observed in simulations and is consistent with experimental data.[4,5] From a purely theoretical point of view, the Debye−Hückel potential exhibits consistent behavior for all distances, and the only issue is whether at short distances it handles aspects like local dielectric constant and molecular structure with accuracy sufficient for one's purposes.

The counterion−polymer potential of mean force is the work required to bring a counterion from infinity to r; so, in addition to the work terms evaluated at r as above, we also need the corresponding terms when the counterion is at infinity. The intrapolymer electrostatic free energy with the counterion at infinity is denoted by $w_p(\infty)$, and is given by eq 5 with $\theta(r)$ replaced by $\theta(\infty)$. Similarly, $w_{\text{transfer}}(\infty)$ is the same as $w_{\text{transfer}}(r)$ in eq 6 but with the replacements $\theta(\infty)$ and $Q(\infty)$ for $\theta(r)$ and $Q(r)$, respectively. Since $K_0(\infty) = 0$, $w_{cp}(\infty)$ vanishes. Denoting the counterion−polymer potential of mean

force simply by w, we then have

$$w(r) = w_p(r) + w_{transfer}(r) + w_{cp}(r) - w_p(\infty) - w_{transfer}(\infty) \quad (8)$$

Since the quantities $\theta(\infty)$ and $Q(\infty)$ pertain to a polymer with the counterion fixed at infinity, they are identical to the corresponding quantities for an isolated polymer in 1:1 electrolyte. From previous work,[2] the optimized (free energy minimized) values are known to be given by the formulas

$$\theta(\infty) = 1 - \xi^{-1} \quad (9)$$

and, with L_{Av} Avogadro's number,

$$Q(\infty) = 8\pi e L_{Av}(\xi - 1)b^3 \quad (10)$$

respectively, if the polymer charge density exceeds the threshold value $\xi = 1$. Recall[2,3] that the simple expression for Q masks the detailed structure and local energetics of the condensed layer, which involve the local structure of the solvent molecules near the chain and the molecular structure of the polymer itself. Equation 10 states that the various detailed contributions to the internal partition function must be consistent with the long-range electrostatic interaction of the condensed layer and Debye−Hückel atmosphere, as expressed by the right-hand side. Note, for example, that the factor $\xi - 1$ in $Q(\infty)$ is the linear charge density of the condensed layer (it vanishes for $\xi = 1$, the threshold value of the polymer charge density below which there is no condensed layer). If in a simple model Q is interpreted as the volume of the condensation region containing a uniform distribution of condensed counterions, it follows from the temperature dependence of ξ that the condensation region *swells* at lower temperatures (for a fixed dielectric constant) to compensate for the increased charge density.

2.2.2. The Optimized Potential. We optimize the counterion−polymer potential $w(r)$ by minimizing the right-hand side of eq 8 with respect to $\theta(r)$. Following the procedure familiar in counterion condensation theory,[2,6] the terms of the left-hand side of the equation $\partial w(r)/\partial\theta(r) = 0$ are grouped into $\ln c$ and constant terms, and these independent classes of terms are separately required to vanish. In this way, we obtain optimized formulas for both the number of condensed counterions $\theta(r)$ and the internal partition function of the condensed layer $Q(r)$. The optimized potential is then obtained by substituting these expressions back into eq 8. In the results listed below, we assume a bare polymer charge density greater than the threshold for condensation, $\xi > 1$.

Near Region. For values of r in the near region, κr is small, and we use eq 4 to represent $K_0(\kappa r)$ in eq 7. Since $\ln \kappa = \text{const} + (1/2) \ln c$, the $\ln \kappa$ term in eq 4 contributes to the class of $\ln c$ terms and acts to perturb the number of condensed counterions from its value for the isolated polymer. The $\ln r$ term in eq 4 is treated as a constant, since points r in the near region are indeed asymptotically constant. The $\ln r$ term therefore appears in the optimized result for the condensed layer partition function, rendering $Q(r)$ dependent on the presence of the counterion at r. This result shows that the potential of mean force from counterion condensation theory is not a mean-field potential.

The result for $\theta(r)$ in the near region is most transparent when presented as multiplied by P, the number of charges on the polymer, since $P\theta$ is the number of counterions condensed on the chain,

$$P\theta(r) = P(1 - \xi^{-1}) - Z \quad (11)$$

Comparison with eq 9 indicates that when a charge of absolute valence Z and sign opposite to the polymer charges is moved from infinity to a point anywhere in the near region, Z univalent counterions are released from the condensed layer, leaving the net charge on the polymer invariant. It is this property of the near region that leads us to identify it with the region occupied by the condensed counterions.

The expression for $Q(r)$ if r is in the near region is

$$Q(r) = 8\pi e L_{Av} b^3 \left[\xi\left(1 - \frac{Z}{P}\right) - 1\right]\left(\frac{re^{\gamma}}{2b}\right)^{-2Z\xi/P} \quad (12)$$

and when eqs 11 and 12 are substituted into eq 8, an optimized expression for the counterion-polymer potential emerges,

$$Z^{-1}w(r) = 2\xi \ln\left(\frac{r}{2b}\right) + 2\ln(\kappa b) + 2\xi\gamma + 1 \quad (13)$$

The $\ln r$ dependence indicates an unscreened attractive interaction between counterion and polymer.

Intermediate Region. Intermediate values of r, defined by eq 1, are larger than near values, but κr remains small. We may continue to use eq 4 for the Bessel function, which for intermediate r reads

$$K_0(\kappa r) \approx -(1 - x)\ln(\kappa r_0) + \ln 2 - \gamma \quad (14)$$

Note that we do not use eq 3 for r_0 in this asymptotic expansion for small κ. In eq 14, r_0 is a fixed distance independent of the asymptotic limit $\kappa \to 0$, whereas eq 3 provides a reasonable numerical estimate for r_0 corresponding to a fixed numerical value of κ. Recall that when the parameter x in eq 14 progressively takes values from 0 to 1, the intermediate range is swept out from $r = r_0$ to $r = \kappa^{-1}$.

The $\ln \kappa$ term in eq 14 contributes to the class of $\ln c$ terms in the minimization condition for the potential, and hence, affects the number of condensed counterions. The constant terms have an influence on the condensed layer partition function. Both the number of condensed counterions and the condensed layer partition function are made dependent on distance r as x sweeps from 0 to 1. The result for the number of condensed counterions $P\theta$ is

$$P\theta(r) = P(1 - \xi^{-1}) - Z(1 - x) \quad (15)$$

This equation indicates that when a Z-valent charge of sign opposite to the polymer charge is brought from the far end of the intermediate region ($x = 1$, $r = \kappa^{-1}$) to its near end ($x = 0$, $r = r_0$), the number of counterions released from the condensed layer into bulk solution increases progressively with approaching distance from 0 to Z. The simple linear dependence on x masks a somewhat more complicated dependence on r through inversion of eq 1. The formula for the condensed layer partition function when the counterion at r is in the

intermediate range is given by

$$Q(r) = 8\pi e L_{Av} b^3 \left\{ \xi \left[1 - \frac{Z}{P}(1-x) \right] - 1 \right\} \left(\frac{r_0^{1-x} e^{\gamma}}{2b^{1-x}} \right)^{-2Z\xi/P} \quad (16)$$

and the intermediate-range counterion-polymer potential $w(r)$ works out to be

$$Z^{-1}w(r) = 2\xi \ln\left[\frac{1}{2} \left(\frac{r_0}{b} \right)^{1-x} \right] + 2\xi\gamma + 2(1-x)\ln(\kappa b) + 1 - x \quad (17)$$

Far Region. In the far range of separation distances, where r is on the same order as the Debye length, the product κr is asymptotically constant. Therefore, the Bessel function $K_0(\kappa r)$ appearing in the optimization condition on the potential is treated as a constant and contributes only to the class of terms that are constant. It does not contribute to the ln c class of terms, and thus, the presence of the counterion at far r does not affect the number of counterions condensed on the polymer. It does, however, perturb the local energetics and structure of the condensed layer as embodied in the consistency condition for the condensed layer partition function. Specifically, we find for the far region a distance-independent unperturbed value for $\theta(r)$,

$$\theta(r) \equiv \theta(\infty) = 1 - \xi^{-1} \quad (18)$$

but a distance-dependent partition function,

$$Q(r) = Q(\infty) \exp[(2Z\xi/P)K_0(\kappa r)] \quad (19)$$

where $Q(\infty)$ is given in eq 10.

Calculation of the counterion-polymer potential in the far region yields an unexpected result,

$$Z^{-1}w(r) = -2\xi K_0(\kappa r) \quad (20)$$

that is, the pair potential in the far region is *exactly* a linear Debye−Hückel interaction, governed by the bare charge density ξ, instead of the anticipated renormalized charge. When we trace through the derivation, we can see what has happened. There is a condensed layer consistent with eq 18. The polymer charge is indeed renormalized, with consequent weakening of the attractive potential. There is an opposing effect of the condensed layer, however. The condensed layer partition function is perturbed by the counterion at r, increasing in accordance with eq 19, and thus enhancing the attraction. These two effects are easily seen to cancel exactly in the calculation, and the condensed counterions finally have no net effect on the far-region potential. Similarly opposing effects have been found for the polymer−polymer pair potential at far separation distances between parallel polymer segments,[6] but in that case, cancellation is not complete, and the result is a potential nonlinear in ξ.

We can also suggest a physical interpretation of the increase of the internal partition function of the condensed layer caused by the presence of a counterion fixed at a far distance r. A simplified but intuitive interpretation of the condensed layer partition function is that it equals the volume occupied by the condensed counterions.[6] The counterion at r is engaged in repulsive electrostatic interaction with the condensed counterions, so, in this sense, the condensed layer together with the counterion at r may be conceptualized as a generalized condensed layer. The generalized layer has a higher self-repulsive charge density than the isolated physical layer (which is exclusive of the counterion at r). The counterion at r is *fixed* there and cannot contribute to structural rearrangement of the generalized layer in response to the increased charge density. So, in response to the augmented charge density, the volume of the physical condensed layer expands.

Numerical Illustrations. We have three asymptotic formulas for $w(r)$, eqs 13, 17, and 20, each pertaining to a separate region of asymptotic space, the near, intermediate, and far ranges, respectively. The regions do not overlap (all distances in the near region are smaller than intermediate distances, and all far distances are larger than intermediate). Thus it appears that we may have no mechanism for rigorously connecting the three components of the potential. Nonetheless, we have identified an approximate boundary point r_0 between the near and intermediate ranges, given by eq 3 for a fixed value of κ, and the formulas for near and intermediate $w(r)$ are indeed mutually continuous across this boundary. By setting $x = 1$ in eq 1, we also find the reasonable estimate $r = 1/\kappa$ for a boundary between intermediate and far ranges, but in this case, the expressions for intermediate and far potentials are not continuous across the boundary. From the standpoint of pure theory, use of the asymptotic expansion eq 4 for $K_0(\kappa r)$ in the near and intermediate asymptotic ranges but not in the far range may be correct but does lead to an unrealistic jump in graphical representations of the potential for specific (i.e., nonasymptotic) numerical values of κ and r.

It is not difficult to remedy this situation, albeit at the cost of some further approximation. Equation 20 for the far potential is already expressed in terms of $K_0(\kappa r)$. We modify eqs 13 and 17 by substituting $K_0(\kappa r)$ in place of terms in them that we identify as the asymptotic representation of $K_0(\kappa r)$ given by the right-hand side of eq 4. An easy way to make this transformation is to regard eq 4 as a formal equation, solve it formally for the Euler constant γ, and substitute the resulting expression for γ into eqs 13 and 17. For our numerical work, we then get pairwise continuous representations of the potential. In the near region,

$$Z^{-1}w(r) = -2\xi K_0(\kappa r) - 2(\xi - 1)\ln(\kappa b) + 1 \quad (21)$$

In the intermediate range,

$$Z^{-1}w(r) = -2\xi K_0(\kappa r) - 2(1-x)(\xi - 1)\ln(\kappa b) + 1 - x \quad (22)$$

In the far range (same as eq 20),

$$Z^{-1}w(r) = -2\xi K_0(\kappa r) \quad (23)$$

In eq 22, x is a function of r obtained by inverting eq 1, and then using eq 3 for r_0,

$$x(r) = 1 + \ln(\kappa r) \quad (24)$$

The "continuity transformation" that generates eqs 21−23 does not qualitatively affect the interesting behavior noted below in the near and intermediate ranges. In all illustrations shown, the counterion at r is univalent ($Z = 1$), $c = 0.01$ M ($1/\kappa = 30.4$ Å), and $b = 1.7$ Å ($\xi = 4.2$). Recall that $w(r)$ is expressed in units of $k_B T$.

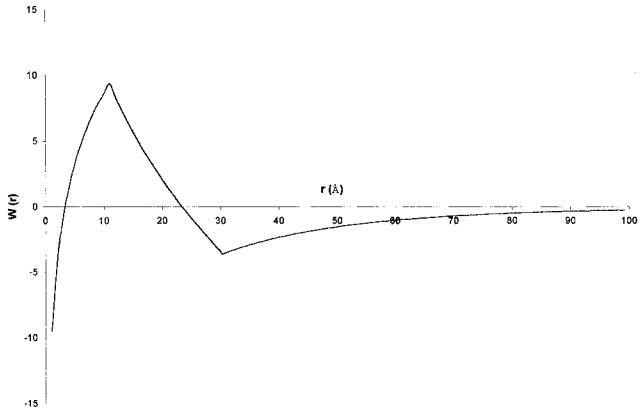

Figure 1. Counterion−polymer potential of mean force. Counterion valence $Z = 1$, polymer charge spacing $b = 1.7$ Å, reduced charge density $\xi = 4.2$, salt concentration $c = 0.01$ M, and Debye screening length $\kappa^{-1} = 30.4$ Å. Near region from 0.85 to 11.2 Å, intermediate region from 11.2 to 30.4 Å, and far region from 30.4 Å to infinity.

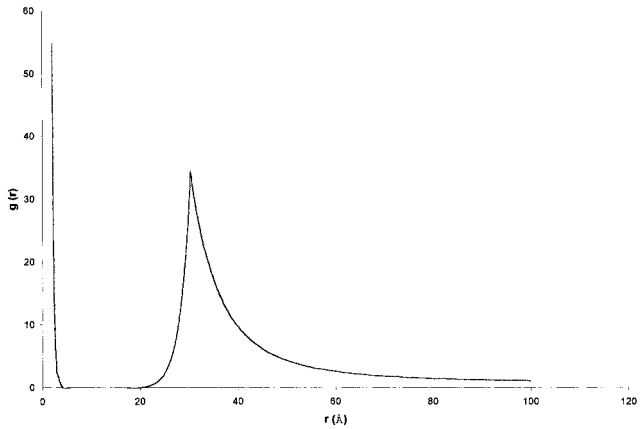

Figure 2. Counterion radial distribution function. Parameters as in Figure 1.

Figure 1 illustrates the counterion−polymer pair potential $w(r)$. Unrealistic cusps at the near−intermediate and intermediate−far boundaries reflect the approximate nature of the joining conditions. The attraction in the far region is numerically unremarkable. The attractive branch in the near region crosses the energy axis into positive values, and the intermediate branch features a repulsive interactive force. A counterion penetrating close to the polymer must first cross a steep energy barrier.

Figure 2 shows the counterion−polymer radial distribution function, $g(r) = \exp[-w(r)]$. The local concentration of counterions nearly vanishes in the region of the repulsive barrier in the potential. Two populations of counterions, a compact condensed layer and a diffuse Debye−Hückel cloud, are manifest.

Figure 3 is a plot of the integrated counterion charge, $I(r) = 2\pi bc \int_a^r rg(r)\,\mathrm{d}r$. This quantity gives the amount of counterion charge (for each of the P polymer charges) contained between some cut-off distance of closest approach a and variable distance r. $I(r)$ is sensitive to the choice of a, and we have fixed a by requiring that the plateau conspicuous in Figure 3 have the level value $1 - \xi^{-1} = 0.76$, that is, the charge per polymer charge contained in the condensed layer. With this requirement, $a = 0.85$ Å. It is easy to prove directly from the formulas involved that the value of a is only slightly dependent on the ionic strength c (because of the dependence on c of the outer boundary r_0 of the condensed layer), but it is rather more sensitive to the polymer charge density. The plateau in the interface between the condensed layer and the diffuse cloud signifies that counterion charge does not accumulate in this region.

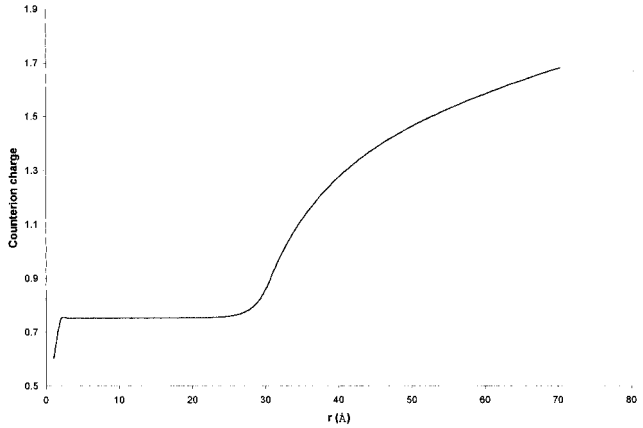

Figure 3. Unsigned counterion charge enclosed within distance r per polymer charge. Parameters as in Figure 1.

2.3. Coion−Polyion Potential. It might be thought that the coion−polymer potential is simply the negative of the counterion−polymer potential, and this result is indeed the one obtained if we change the sign of the right-hand side of eq 7, while, apparently reasonably enough, retaining identically all other components of the work from the counterion analysis. Setting the coion potential equal to $-w(r)$ turns out not to be physically meaningful, however, because if we use this expression to calculate the total charge outside the polymer, we get a result far from the value needed to neutralize the polymer charge.

On reflection, we reasoned as follows for a univalent coion at r in the near region, which is the region occupied by the condensed counterions. When a coion penetrates the condensed layer, it becomes part of the net charge of the polymer. Having the same sign as the P structural polymer charges, the coion cooperates on an equal basis with them in the determination of the number of condensed counterions. The coion potential is then not expected to equal the negative of the counterion potential, because a coion fixed at r is partially associated (with condensed counterions), while a counterion fixed at r is unassociated. Yet again, a coion in the near region is exposed to a high local concentration of counterions, but a counterion in the near region finds very few coions. Even more generally stated, our theory is highly nonlinear, and an asymmetric relation between counterion and coion is no surprise.

Let θ be the number of condensed counterions per polymer and coion charge, so that $(P + 1)\theta$ is the number of condensed counterions associated with the polymer−coion complex. In this model, the polymer is a linear array of P renormalized charges $(1 - \theta)q$ with spacing b, and the coion fixed in the near region also bears renormalized charge $(1 - \theta)q$. The discussion of the work components now proceeds in straightforward fashion. The intrapolymer repulsions among renormalized charges continues to be given by eq 5 but with a modified meaning of θ as indicated. Since $(P + 1)\theta$ counterions are transfered from bulk to condensed layer, eq 6 holds over with the factor P replaced by $P + 1$. The

interaction between polymer and coion at r takes the form

$$\bar{w}_{cp}(r) = 2\xi(1 - \theta)^2 K_0(\kappa r) \tag{25}$$

since the coion also has a renormalized charge (we use bars to indicate work terms in the coion-polymer case). The reference terms at infinity are the same as before, and in eq 10, $\theta(\infty)$ has its previous meaning as P^{-1} times the number of counterions condensed on the isolated polymer.

The standard procedure for minimizing the work goes through without difficulty, and the first result we obtain is that $\theta(r)$ in the near region is given by a constant value,

$$\theta = 1 - \frac{P + 1}{\xi(P + 2)} \tag{26}$$

The meaning of this formula is clarified by an expansion of the right-hand side in powers of P^{-1} with disposal in the long polymer limit of terms of order P^{-2} and higher. We then find to leading order,

$$(P + 1)\theta = P(1 - \xi^{-1}) + 1 \tag{27}$$

that is, the total number of condensed counterions is increased by one when a coion penetrates the condensed layer. The net charge of the polymer, condensed counterions, and coion is the same as for the isolated polymer with its condensed layer.

The result for the condensed layer partition function $Q(r)$, r in the near region, is

$$Q(r) = 8\pi e L_{Av} b^3 \left(\xi - \frac{P + 1}{P + 2}\right)\left(\frac{re^{\gamma}}{2b}\right)^{4/(P+2)} \tag{28}$$

Finally, in the near region, the pair potential $\bar{w}(r)$ for coion and polymer is calculated (with the continuity transformation) as

$$\bar{w}(r) = 2(2 - \xi^{-1})K_0(\kappa r) + 2(1 - \xi^{-1}) \ln(\kappa b) - 1 \tag{29}$$

A coion in the far region should behave like an ion in the Debye−Hückel cloud. It is not to be regarded as part of the net charge of the polymer and has no condensed counterions associated with it. In this region, therefore, $\bar{w}(r)$ is equal to the negative of $w(r)$, as given by eq 20,

$$\bar{w}(r) = 2\xi K_0(\kappa r) \tag{30}$$

The number of counterions condensed on the polymer when a coion is fixed in the far region is the same as that for an isolated polymer, as indicated by eq 18. The result for the condensed layer partition function is similar to that for eq 19 but with a sign change,

$$Q(r) = Q(\infty) \exp[(-2\xi/P)K_0(\kappa r)] \tag{31}$$

where $Q(\infty)$ is given by eq 10. Like a counterion in the far region, the presence of a coion perturbs the condensed layer.

The intermediate region is a more complicated affair. When the coion is in the near region, it is fully integrated into the polymer charge. When it is in the far region, its charge is entirely apart from the polymer. Therefore, the charge of a coion in the intermediate region is partially integrated into the polymer charge.

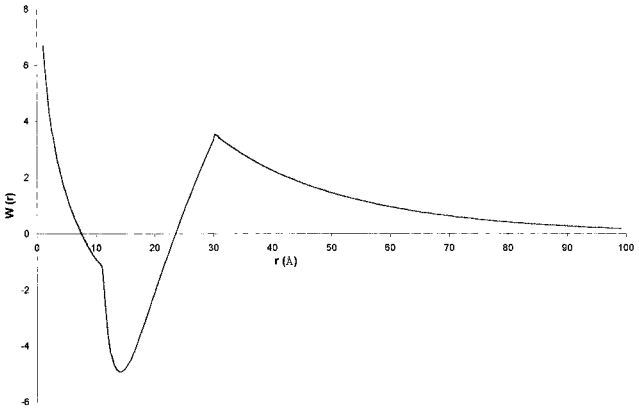

Figure 4. Coion−polymer potential of mean force. Parameters as in Figure 1.

The polymer continues to be a linear array of renormalized charges $q(1 - \theta)$. The coion is assigned the partially renormalized charge $q[1 - \theta f(x)]$, where x is the parameter correlated with position in the intermediate region according to eq 1, and $f(x)$ is a function to be determined. Since $x = 1$ at the intermediate−far boundary, where the charge of the coion is not renormalized, we require that $f(1)$ vanish. Since $x = 0$ at the near−intermediate boundary, where the charge of the coion is fully renormalized, we require $f(0) = 1$.

The work components take into account the transfer of $[P + f(x)]\theta$ counterions from bulk to condensed layer. The direct electrostatic component between coion and polymer has the form

$$\bar{w}_{cp}(r) = 2\xi(1 - \theta)[1 - \theta f(x)]K_0(\kappa r) \tag{32}$$

The optimization procedure involves some lengthy expressions but ultimately yields results. For example, $\theta(r)$ in the intermediate region turns out as

$$\theta(r) = 1 - \frac{1}{\xi} + \frac{f(x)(1 - 2x) + \xi(1 - x)[1 - f(x)]}{P\xi} \tag{33}$$

This formula agrees with the far-region value when $x = 1$ and with the near-region value, to terms of order P^{-1}, when $x = 0$.

For intermediate r, the coion−polymer potential may be written as follows, with x given by eq 24,

$$\bar{w}(r) = 2\{\xi[1 - f(x)] + f(x)(2 - \xi^{-1})\}\, K_0(\kappa r) + 2[(\xi - 1)(1 - x) + xf(x)(\xi - 3 + 2\xi^{-1}) + f(x)(2 - \xi - \xi^{-1})] \ln(\kappa b) - 1 + x + xf(x)(2\xi^{-1} - 1) \tag{34}$$

To get numerical results, we need an explicit formula for the renormalization function $f(x)$. We have not attempted to determine $f(x)$ by optimizing. Instead, we have required that $f(x)$ be chosen such that the total charge from counterions and coions is equal but opposite in sign to the polymer charge. If we assume the form $f(x) = (1 - x)^{\alpha}$, we find numerically that $\alpha = 5.25$ for the parameters considered in the figures, but there is a strong dependence on ionic strength and polymer charge density.

Figure 4 illustrates the coion−polymer potential $\bar{w}(r)$. The unrealistic "corners" evident in the plot at the

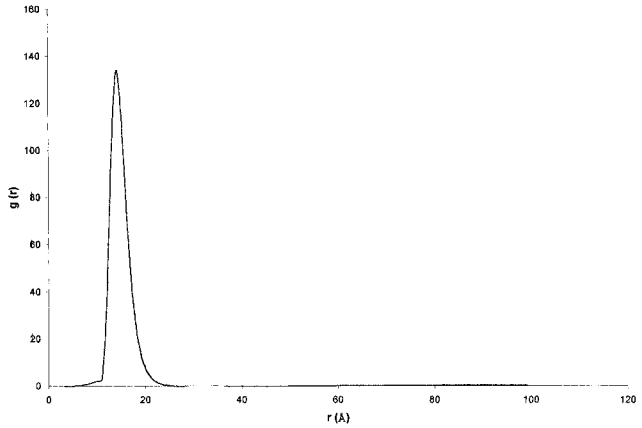

Figure 5. Coion radial distribution function. Parameters as in Figure 1.

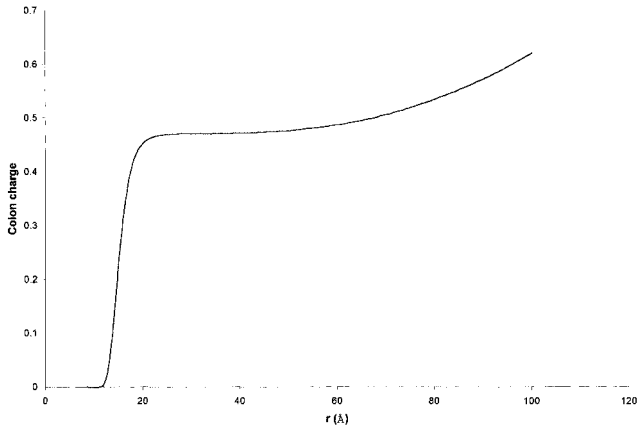

Figure 6. Unsigned coion charge enclosed within distance r per polymer charge. Parameters as in Figure 1.

boundaries between near and intermediate and between intermediate and far regions are symptomatic of our approximate joining conditions. The smooth minimum is interior to the intermediate region. The radial distribution function $\bar{g}(r) = \exp[-\bar{w}(r)]$ in Figure 5 shows a single peak where coions accumulate outside the condensed layer. The integrated (unsigned) charge up to distance r due to the coions is plotted in Figure 6 and indicates significant coion charge in the intermediate region, despite partial renormalization of coion charge by counterion condensation. Finally, we show the net charge due to counterions and renormalized coions together in Figure 7. The polymer has been taken as anionic, and the approach of the curve to the value $+1$ at large distances r signifies neutralization of the polyanion by an excess of positively charged counterions. Since the potentials for both counterion and coion in the far region are of Debye−Hückel type, we linearized the exponentials in the radial distribution functions in this region. In Figure 7 we see the charge outside the polymer rise steeply from 0 to the counterion condensation value 0.76, then level off at this value before dropping as coion charge accumulates. In the final stage, the net charge gradually rises toward the neutralization value unity.

3. Discussion

We have calculated pair potentials for the interaction of counterions and coions with a charged polymer, along with their associated differential and integral distributions. An exponent describing the extent to which a

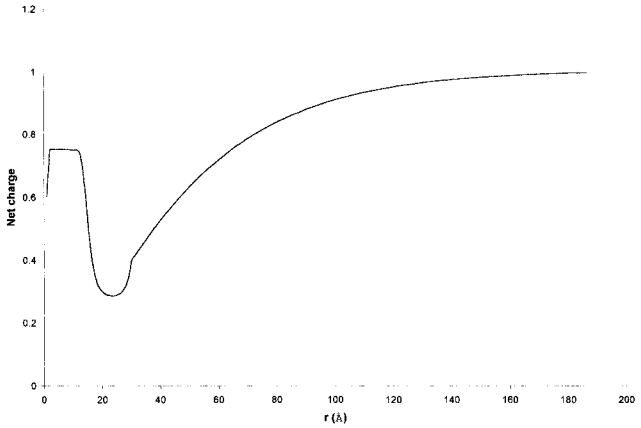

Figure 7. Net charge from counterions and coions enclosed within distance r per negative charge on a polyanion. Parameters as in Figure 1.

coion cooperates with the polymer charges in condensing counterions allows fulfillment of the electroneutrality condition. A hard-core distance between ion and polymer can be chosen to give the correct number of counterions in the condensed layer. Perhaps the most striking result is the two distinct peaks of counterion concentration (Figure 2), the near one corresponding to the condensed layer and the far one located outside a free energy barrier separating the diffuse Debye−Hückel cloud from the condensed layer. A single peak of coion concentration lies between the counterion peaks (Figure 5).

A spatially distinct condensed layer is consistent with a variety of experimental observations, such as charge renormalization, a sharp onset of condensation at a threshold polymer charge density, the invariance of the condensed layer to added salt, and the perturbation of local solvent structure caused by condensation.[1,4] Visual presentation of simulated counterion distributions show a condensed layer spatially distinct from an uncondensed cloud.[5] Our theoretical distributions represent a single polyion immersed in 1:1 electrolyte and cannot be quantitatively compared with simulated data on systems containing only counterions. The entire construction of our theory highlights the Debye length as a length scale of central importance, and a question that should be asked of any simulation is whether the system size and running times have established the Debye length of the solvent.

The structure of our theoretical condensed layer has only a radial component, and the cut-off distance of closest approach is very small. Qualitative comparison with simulation[5] shows the limitations of our approach. A prominent feature of the simulated layer of counterions condensed on DNA is the faithfulness of the counterions to the double-helical trajectory of the charged DNA phosphate groups. Our theoretical counterion distribution can reflect no local polymer structure other than that of our model, a linear array of charged sites. On the other hand, the radial distribution function for the condensed counterions is not too different from the radial distribution of the simulation (averaged over the angular dependence), if our cut-off distance is interpreted as the distance from the DNA surface. In both theory and simulation, the condensed layer is closely associated with the polymer chain, lending support to the understanding of charge renormalization as a physical reduction of the electrostatic charge carried by the chain.

Acknowledgment. The research reported here was sponsored in part by the Public Health Service through Grant GM36284. We are grateful to Nancy Marky for suggesting the "continuity transformation".

References and Notes

(1) Manning, G. S. *Ber. Bunsen-Ges. Phys. Chem.* **1996**, *100*, 909−922.
(2) Manning, G. S. *Physica A* **1996**, *231*, 236−253.
(3) Manning, G. S.; Ray, J. *J. Biomol. Struct. Dyn.* **1998**, *16*, 461−476.
(4) Essafi, W.; Lafuma, F.; Williams, C. *Eur. Phys. J. B* **1999**, *9*, 261−266.
(5) Young, M. A.; Jayaram, B.; Beveridge, D. L. *J. Am. Chem. Soc.* **1997**, *119*, 59−69.
(6) Ray, J.; Manning, G. S. *Langmuir* **1994**, *10*, 2450−2461.
(7) Ray, J.; Manning, G. S. *Macromolecules* **1997**, *30*, 5739−5744.

MA9902091